The Coupling Factor Dependence of Lossy Voice Coil Impedance Based of Transformer Model

Ginn Anazawa

▶ **To cite this version:**

Ginn Anazawa. The Coupling Factor Dependence of Lossy Voice Coil Impedance Based of Transformer Model. Forum Acusticum, Dec 2020, Lyon, France. pp.559-566, ⟨10.48465/fa.2020.0598⟩. ⟨hal-03231980⟩

HAL Id: hal-03231980

https://hal.science/hal-03231980v1

Submitted on 21 May 2021

HAL is a multi-disciplinary open access archive for the deposit and dissemination of scientific research documents, whether they are published or not. The documents may come from teaching and research institutions in France or abroad, or from public or private research centers.

L'archive ouverte pluridisciplinaire **HAL**, est destinée au dépôt et à la diffusion de documents scientifiques de niveau recherche, publiés ou non, émanant des établissements d'enseignement et de recherche français ou étrangers, des laboratoires publics ou privés.

HAL Authorization

THE COUPLING FACTOR DEPENDENCE OF LOSSY VOICE COIL IMPEDANCE BASED OF TRANSFORMER MODEL

Isao G. Anazawa
[1] Ny Works, North Vancouver, British Columbia, Canada
g_anazawa@bell.net

ABSTRACT

This paper presents the lossy voice coil block impedance model using the transformer-based circuitry and introduced two types of lossy impedance modeling the infinite and the finite short-ring. The transformer-based impedance model treats the voice coil self-inductance as the primary winding and the surrounding conductive medium as lossy impedance with frequency dependence of $\sqrt{\omega}$ connected to the secondary winding. The model successfully describes the blocked impedance frequency dependence which agreed at a high degree of accuracy with the actual samples. Also, the model showed intricate connections between the transformer coupling coefficient κ and the magnitude of frequency dependency.

1. INTRODUCTION

A conductor under the conditions of the Eddy current, skin effect, and proximity effect (Eddy Losses), the conductor's impedance increases at the rate of $\sqrt{\omega}$ shown by Cohen [1] and Holtz [2]. The lossy voice coil impedance, however, empirically found that the impedance increases at the rate higher than $\sqrt{\omega}$: Wright [3].

Voice coil impedance without the main resonance, or blocked impedance, was studied and electrical models were developed to describe the lossy impedance characteristics. Those models are using; (i) Semi-inductance by Vanderkooy [4], Thorborg [5], (ii) single or multiple orders of LR parallel network (Foster type) by Klippel [6], Leach [7], [5], (iii) LR ladder network or Cauer type by Thompson [8], and Neves et., al. [9], and (iv) Physical Cauer type by Wheeler et al. [10], Colla [11]. Note that [9] to [11] were studied for the field of power electronics.

While these models successfully implemented the lossy voice coil impedance within a limited frequency range, however, the models do not address why and how the lossy impedance increase with the rate higher than $\sqrt{\omega}$.

In this paper, the voice coil impedance is modeled using a transformer consisting of the voice coil self-inductance as the primary winding. The surrounding conductive mediums are treated as Eddy Losses impedance with a frequency dependence of $\sqrt{\omega}$ connected to the one-turn secondary winding. Resulting simulations were compared for accuracy primarily for micro-speaker samples. However, this model is not limited and is easily applicable to a larger loudspeaker. Note that the treatment of the blocked impedance with the transformer modeling was also done by Thorborg [12], and Elileli [13].

2. LOUDSPEAKER ELECTRICAL MODEL

Figure 1 depicted a loudspeaker electrical model with the transformer representing the electromagnetic coupling of the voice coil and the surrounding conductive mediums.

The model consists of the DC resistance R_E, the self-inductance L_E, and the main physical resonance elements of L_{CES}, C_{MES}, and R_{ES}. The inductance L_E and surrounding conductive material are magnetically coupled and formed a transformer. An inductance L_2 represents the one-turn secondary winding. L_2 is connected to the lossy impedance of Z_{EDY} of which has the frequency dependence of $\sqrt{\omega}$.

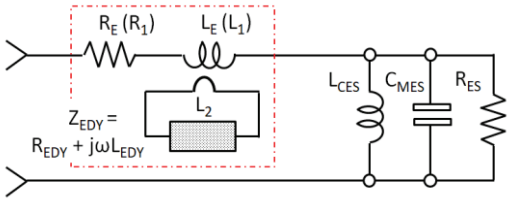

Figure 1– Loudspeaker electrical equivalent model

3. VOICE COIL BLOCKED IMPEDANCE

3.1 Blocked Impedance Characteristics

Figure 2 shows both the blocked impedance and frequency dependence response for a typical 6Ω (R_E = 6.4Ω) sample micro-speaker. A frequency range of 100MHz was used primarily to show where the voice coil self-resonance occurs and influences the impedance and frequency dependence. The self-resonance phenomenon in this sample appeared at approximately 21MHz.

The entire blocked impedance frequency dependence characteristics can be divided into three regions. Region 1 is the frequency range that has insignificant Eddy Losses. Therefore the total impedance can be approximated with the DC resistance of R_E. Region 2 is the frequency range where lossy impedance dominates the total impedance. The impedance is known to follow the Log-log linear relationships [3].

When the impedance increases (decrease) at the rate of ω^{λ}, the frequency dependence denoting λ takes some positive (negative) value. Thus the impedance increases with the rate of $\sqrt{\omega}$ has the frequency dependence of 0.5. The majority of loudspeaker voice coil impedance showed that the frequency dependence is higher than this and around 0.7 to 0.9 [3]. Based on the four voice coil

samples, the average total impedance frequency dependence λ_Z is found to be 0.84.

The frequency dependence λ_Z was obtained by using the arbitrarily selected frequencies ω_L and ω_H within the impedance Log-log linear region, and the corresponding impedances $Z_{(\omega L)}$ and $Z_{(\omega H)}$. Then, taking the ratio of the impedance difference over the frequency deference in logarithmic expression, the frequency dependence is obtained by using the following equation.

$$\lambda_Z = \frac{\mathrm{Log}\left(\frac{|Z_{(\omega H)}|}{|Z_{(\omega L)}|}\right)}{\mathrm{Log}\left(\frac{\omega_H}{\omega_L}\right)}$$

Region 3 is the frequency range that is dominated by the voice coil self-resonance. The self-resonance that is appeared at 20.9MHz, is caused by the self-inductance L_E and the parasitic capacitance within the voice coil windings forming a resonant circuit.

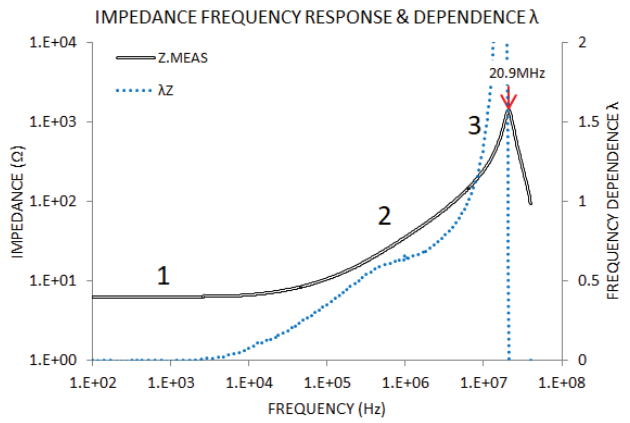

Figure 2 – Sample #7.4 voice coil blocked impedance and the impedance frequency dependence: The impedance is shown in black and the frequency dependence is shown in blue traces.

3.2 Frequency Range

The upper-frequency limit for the tests is determined by the following two facts.

First, the higher the frequency limit is better characterizing the lossy impedance where Eddy Losses dominates. However, the frequency range is limited by a frequency where the voice coil's self-resonance phenomenon appears. The parasitic capacitance denoting as C_P and the voice coil self-inductance L_E forms an LC parallel circuit and the resonance frequency ω_{SR} given by $1/\sqrt{L_E{}'C_P}$. L_E' is a reduced value of L_E and the reduction occurs due to Eddy Losses. The self-resonance frequencies of the samples were found as low as 10MHz and as high as 20MHz. For these tested samples, an upper- frequency limit that those impedance responses are free from the self-resonance is determined as 1MHz or 1/10th of the self-resonance frequency.

Second, the frequency dependence response showed as the dotted blue trace in Figure 2, is monotonically increased from 4kHz up to 600kHz. The impedance Log-log region exists only between adjacently above and below the 1/10th (or 2MHz) of the self-resonance.

When using the Wright model [3] for the impedance simulation, two reasonably separated frequencies have to be set ideally within Log-log linear region.

The model expresses lossy impedance components as $R_\omega = K_R\omega^{\lambda_R}$ for real impedance and $L_\omega = K_L\omega^{\lambda_L}$ for the inductance. From these expressions, the total impedance excluding DC component R_E can be similarly expressed as $Z_\omega = K_Z\omega^{\lambda_Z}$.

As an example, the lower sampling frequency ω_L set at the frequency where the impedance becomes $|Z_{VC}(\omega_L)| = 3R_E$, and higher frequency ω_H is set where the impedance is $|Z_{VC}(\omega_H)| = 2x|Z_{VC}(\omega_L)|$. The higher sampling frequency ω_H is calculated as approximately 1.14MHz. Note that parameters used are from the sample #7.4 shown in Figure 2; the corner frequency ω_C is 60kHz, ω_L is 6 times of the ω_C, and the impedance frequency dependence λ_Z is derived as 0.6.

$$\omega_H = \omega_L\left(\frac{Z_{VC}(\omega_H)}{Z_{VC}(\omega_L)}\right)^{\frac{1}{\lambda_Z}}$$

Note: All tested samples were measured up to 100MHz for the reason of determining the influence of self-resonance on the measurements. Some test results were shown up to 100MHz for the benefit of explanation for voice coil frequency dependency. Determining the voice coil transformer coupling coefficient (or factor) κ, the frequency range has to extend above 1MHz as explained in section 4.3. The low-frequency limits were set at 100Hz that is lower than the main physical resonance frequency.

3.3 Lossy Impedance Z_{EDY}

The lossy impedance denoting as Z_{EDY} has a frequency dependence of $(1+j)\sqrt{\omega}$ [4], [15]. This can be interpreted as the impedance consists of serially connected real (R_{EDY}) and imaginary impedance (X_{EDY}), and the frequency dependence of 0.5.

$$Z_{EDY} \propto \sqrt{j\omega} = \frac{1+j}{\sqrt{2}}\sqrt{\omega}$$

The R_{EDY}, X_{EDY} and L_{EDY} (= X_{EDY}/ω) can be expressed as follows; the real impedance R_2 and the inductance L_3 are the values defined at the normalized frequency ω_0.

$$Z_{EDY} = R_{EDY} + jX_{EDY} = R_{EDY} + j\omega L_{EDY} \quad (1)$$

$$R_{EDY} = R_2\sqrt{\frac{\omega}{\omega_0}} \quad (2)$$

$$L_{EDY} = L_3\sqrt{\frac{\omega_0}{\omega}} \quad (3)$$

The transformer-based blocked impedance electrical model is shown in Figure 3. Parameters are transformer primary inductance of L_1 (= L_E), voice coil DC resistance R_1 (= R_E), transformer secondary inductance L_2

terminated with the lossy impedance Z_{EDY}. The mutual inductance is denoted as M, the input voltage as V_1, primary circuit current as I_1 and the secondary winding's current as I_2. Kirchhoff's Voltage Law is applied to the primary and secondary circuits of the transformer, and that is expressed as (4).

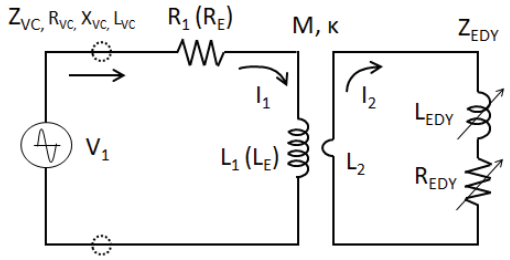

Figure 3 – Blocked voice coil impedance transformer model including Eddy Losses impedance Z_{EDY}

$$\begin{bmatrix} V_1 \\ 0 \end{bmatrix} = \begin{bmatrix} R_1 + j\omega L_1 & -j\omega M \\ -j\omega M & j\omega L_2 + Z_{EDY} \end{bmatrix} \begin{bmatrix} I_1 \\ I_2 \end{bmatrix} \quad (4)$$

By expanding (4) for the total impedance Z_{VC} (= V_1/I_1), its real part Re(Z_{VC}) or R_{VC} and its inductance Im(Z_{VC})/ω or L_{VC} are derived as (5) and (6) respectively.

$$Z_{VC} = \frac{V_1}{I_1} = R_{VC} + j\omega L_{VC}$$

$$R_{VC} = R_1 + \frac{R_{EDY} M^2}{\left(\frac{R_{EDY}}{\omega}\right)^2 + (L_2 + L_{EDY})^2} \quad (5)$$

$$L_{VC} = L_1 - \frac{(L_2 + L_{EDY})\, M^2}{\left(\frac{R_{EDY}}{\omega}\right)^2 + (L_2 + L_{EDY})^2} \quad (6)$$

The mutual inductance M and the primary and secondary inductance, L_1 and L_2 respectively, and the coupling coefficient κ have the following relationship:

$$M = \kappa \sqrt{L_1 L_2} \quad (7)$$

I_1	Primary windings closed current
I_2	Secondary windings closed current
L_1	Primary windings inductance (L_E)
L_2	Secondary windings inductance
L_{EDY}	Eddy Losses inductance
L_{VC}	Input inductance
L_{MIN}	Minimum inductance
M	Mutual inductance
R_1	Voice coil resistance (R_E)
R_2	Secondary winding resistance
R_{EDY}	Eddy Losses real impedance
R_{VC}	Input real impedance
X_{VC}	Input imaginary impedance
Z_{EDY}	Eddy Losses impedance
Z_{VC}	Input impedance
κ	Transformer coupling coefficient
ω	Angular frequency (rad/s), ω = 2πf
ω_0	Normalized frequency
ω_{SR}	Voice coil's self-resonance frequency

4. VOICE COIL BLOKED IMPEDANCE PARAMETERS

4.1 Impedance Frequency Dependency

At sufficiently high-frequency ω where the real impedance $R_{VC}(\omega)$ and the inductance $L_{VC}(\omega)$ frequency dependency holds a Log-log linear relationship, the impedance components (5) and (6) are asymptotically simplified [17] as follow:

$$R_{VC(\omega)} \simeq R_1 + q\kappa^2\sqrt{\omega} \quad (8)$$

$$L_{VC(\omega)} \simeq \frac{L_1\left[L_3\sqrt{\omega_0}(2-\kappa^2) + L_2(1-\kappa^2)\sqrt{\omega}\right]}{2L_3\sqrt{\omega_0} + L_2\sqrt{\omega}} \quad (9)$$

$$p = \frac{L_1 L_3}{L_2}\sqrt{\omega_0}, \qquad q = \frac{L_1 R_2}{L_2\sqrt{\omega_0}} \quad (10)$$

$$\omega_0 = \frac{R_2}{L_2 + L_3}$$

From real impedance (8) and inductance (9), the total impedance Z_{VC} and the phase φ can be expressed as follows:

$$|Z_{VC}| = \sqrt{R_{VC}^2 + X_{VC}^2} = \sqrt{R_{VC}^2 + (\omega L_{VC})^2}$$

$$\simeq \sqrt{\left(R_1 + q\kappa^2\sqrt{\omega}\right)^2 + \omega^2\left[\frac{L_1 L_3\sqrt{\omega_0}(2-\kappa^2) + L_1 L_2(1-\kappa^2)\sqrt{\omega}}{2L_3\sqrt{\omega_0} + L_2\sqrt{\omega}}\right]^2}$$

$$\simeq \sqrt{\left(R_1 + q\kappa^2\sqrt{\omega}\right)^2 + \left[p(2-\kappa^2)\sqrt{\omega} + L_1(1-\kappa^2)\omega\right]^2} \quad (11)$$

$$2L_3\sqrt{\omega_0} \ll L_2\sqrt{\omega} \quad (12)$$

$$\varphi = \tan^{-1}\frac{X_{VC}}{R_{VC}} = \tan^{-1}\frac{\omega L_{VC}}{R_{VC}} \quad (13)$$

4.2 Impedance Frequency Dependence Higher than 0.5

By taking both the lowest (= 0) and highest (= 1) limits of the coupling coefficient κ, and applying this to (8) for the real impedance $R_{VC}(\omega)$, to (9) for the inductance $L_{VC}(\omega)$, and to (11) for the impedance $Z_{VC}(\omega)$, these impedance components can be expressed in terms of κ as follows:

$$R_{VC(\omega)} \simeq R_1|^{\kappa=0} \sim q\sqrt{\omega}\,|^{\kappa=1} \quad (15)$$

$$L_{VC(\omega)} \simeq L_1|^{\kappa=0} \sim \frac{p}{\sqrt{\omega}}\Big|^{\kappa=1} \quad (16)$$

$$|Z_{VC(\omega)}| \simeq L_1\omega\,|^{\kappa=0} \sim \sqrt{q^2+p^2}\sqrt{\omega}\,\Big|^{\kappa=1} \quad (17)$$

$$R_1 \ll L_1\omega \text{ and } q\sqrt{\omega} \quad (18)$$

When κ is 1, the primary and the secondary windings are magnetically perfectly coupled without any leakage inductance. Under this condition, from (15), (16) and (17), the real impedance R_{VC} and the total impedance Z_{VC} has a frequency dependence of $\sqrt{\omega}$, and the inductance is $1/\sqrt{\omega}$. Therefore the imaginary impedance X_{VC} frequency dependence is immediately obtained as $\sqrt{\omega}$. Conversely when $\kappa = 0$, the transformer is in effect without the secondary. Therefore R_{VC} and L_{VC} do not have any frequency dependence, and the impedance Z_{VC} has frequency dependence of ω as expressed in (17).

The transformer-based model simulation of the impedance, the inductance, and the phase response are shown through Figure 4 through 7. The voice coil impedance parameters are taken from sample #1.2. As simulations shown in the figures, the coupling coefficient κ increased from 0 to 1, the frequency dependence of real impedance R_{VC} monotonically shifts from none to $\sqrt{\omega}$. Similarly the inductance L_{VC} shifts from none to $1/\sqrt{\omega}$ and Z_{VC} shifts from ω to $\sqrt{\omega}$. Within the high range of coupling coefficient ($\kappa = 0.8 \sim 1$), the deviation of the real impedance R_{VC} frequency dependence is rather minimal as shown in Figure 4. On the other hand, as shown in Figures 5 and 6, the inductance L_{VC} frequency dependence deviates significantly by the varying κ, as are the imaginary impedance X_{VC} (= ωL_{VC}, not shown), and the total impedance Z_{VC}.

The phase response simulation shown in Figure 7, the phase φ is settled at approximately 40◦ when κ is set as 1. It is important to note that when the coupling coefficient κ is less than 1, the phase φ always approaches the maximum value of 90◦ at some high frequency. Only when κ is 1, the phase φ limits at some magnitude less than 90◦. Only if the voice coil real and imaginary impedance, R_{VC} and X_{VC} respectively, are equal, the phase φ becomes 45◦.

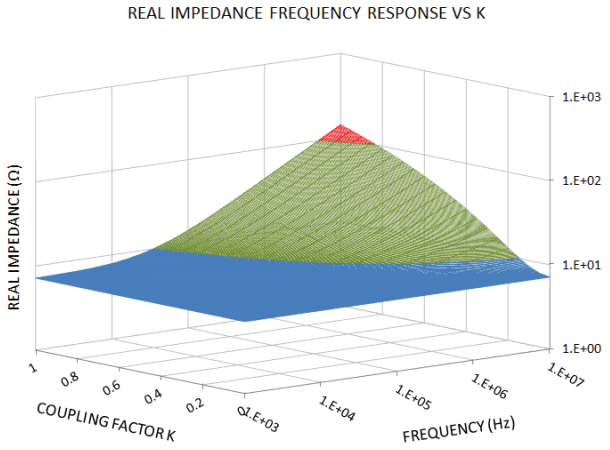

Figure 4 - Simulated real impedance R_{VC} response with varying coupling coefficient κ. Note that the order of κ is reversed compared with Figure 6 through 8 for better visibility.

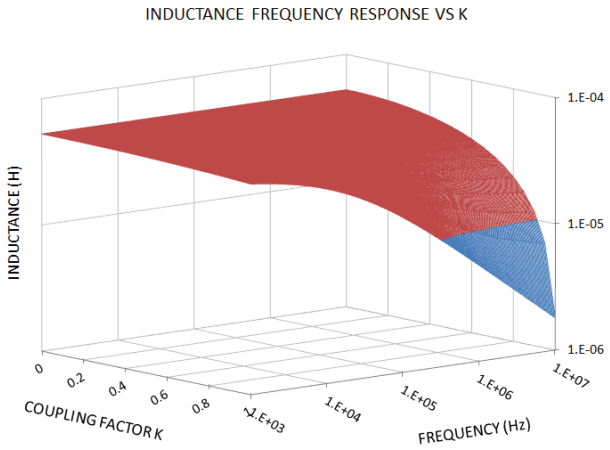

Figure 5 - Simulated inductance L_{VC} response with varying coupling coefficient κ

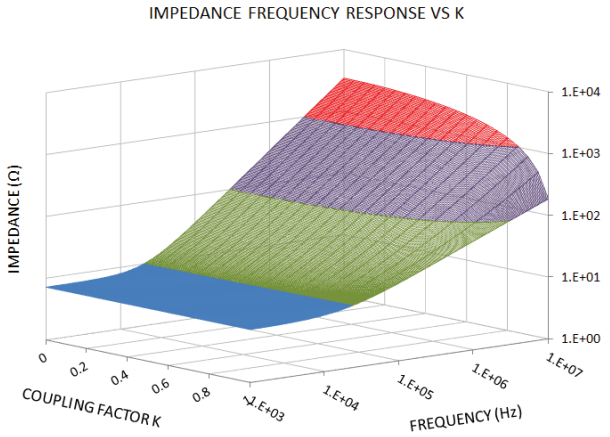

Figure 6 - Simulated total impedance Z_{VC} response with varying coupling coefficient κ

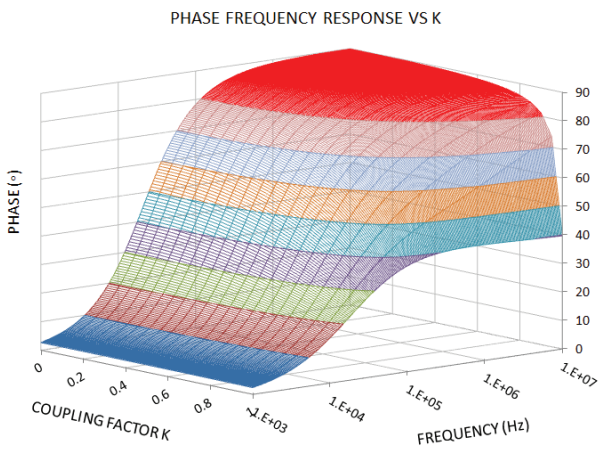

Figure 7 - Simulated phase response with varying coupling coefficient κ

Table 1 summarized the simulation results of the coupling coefficient κ impacting frequency dependence.

It shows the frequency dependence for real impedance λ_R, the inductance λ_L, and the total impedance λ_Z. For the imaginary impedance λ_X is immediately obtained from following relationship: $\lambda_X = \lambda_L + 1$ ($X(\omega) = \omega L \omega^{\lambda L} = L\omega^{(\lambda L+1)}$). In summary, when the coupling coefficient κ is 1, the frequency dependencies are 0.5 for the real, the imaginary and the total impedance, or -0.5 for the inductance.

Conversely, even a slight decrease of κ from the maximum value of 1, the inductance frequency dependence is significantly altered, therefore imaginary impedance and the total impedance. On the other hand, the real impedance is only slightly affected by the deviation of κ. Most voice coils are designed with a coupling coefficient less than 1, thus the voice coil total impedance frequency dependence is higher than 0.5 (and smaller than 1).

FREQUENCY DEPENDENCE			
κ	λ_R	λ_L	λ_Z
1.0	0.497	-0.453 (-0.498*)	0.503
0.9	0.475	-0.228	0.772
0.8	0.448	-0.136	0.886

Table 1 – List of frequency dependence factor of real impedance λ_R, inductance λ_L and total impedance λ_Z. The values were obtained while varying coupling coefficients κ. Two sampling frequencies ω_1 and ω_2 were derived from $\omega_1 = \omega_2/4$, $\omega_2 = \omega_{SR}/10$. For the exception marked as *, the frequencies ω_1 = 1MHz and ω_2 = 4MHz were used.

4.3 Deriving Coupling Coefficient

While κ is in the range of $0 < \kappa < 1$, the inductance L_{VC} converge to the terminal inductance L_{MIN}, as the frequency goes to sufficiently high. The L_{MIN} is equivalent to the apparent inductance L_{VC} when the secondary is terminated by zero impedance.

$$\lim_{\omega\to\infty} L_{VC} = L_1(1-\kappa^2) = L_{MIN} \tag{19}$$

$$\kappa = \sqrt{1 - \frac{L_{MIN}}{L_1}} \tag{20}$$

From this result, a voice coil coupling coefficient κ can be obtained, from (20), by knowing the L_1 (= L_E) and the terminal inductance L_{MIN}. In actuality, however, it was not possible to obtain L_{MIN} directly for all of the tested voice coils, because the presence of self-resonance makes it impossible to determine L_{MIN}.

Figure 8 shows the inductance response of both the sample voice coil and the simulation. The self-resonance of the sample voice coil appeared at approximately 21MHz, well below the frequency that can be determined for L_{MIN}. Because of this fact, the coupling coefficient κ is derived using a curve fitting method instead. To derive the coupling coefficient κ, the inductance equation (6) is solved for the mutual inductance M. From this κ is immediately obtained using the relationship (7).

$$M = \sqrt{\frac{(L_1 - L_{VC(\omega)})}{L_2 + L_{EDY}}\left[\left(\frac{R_{EDY}}{\omega}\right)^2 + (L_2 + L_{EDY})^2\right]}$$

The simulated responses (dotted black and blue) in the Log-log linear region, of approximately 50kHz up to 700kHz in this sample, was fitted against an actual sample inductance response (solid red).

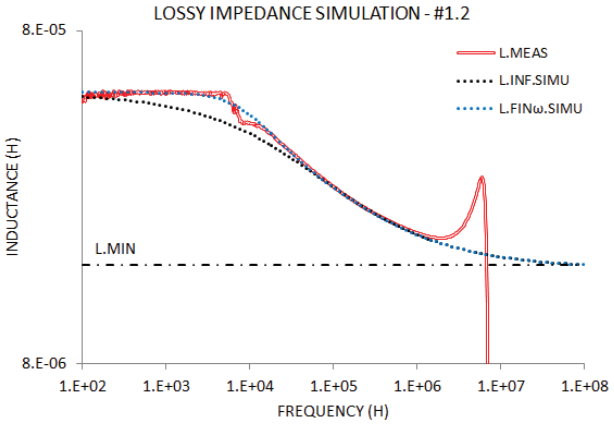

Figure 8 - Voice coil sample #1.2 inductance frequency response: Voice coil #1.2 inductance (red). Two simulations based on infinite model (black dot) and finite model (blue dot), and L_{MIN} (black dash-dot).

Note that two simulations are the infinite (dotted black) and the finite (dotted blue) model. The infinite model significantly deviates the response below 50kHz, however, it yields the same terminal inductance L_{MIN} around 70MHz and higher. The infinite model consists of the impedance components expressed using (2) and (3), the lossy real impedances R_{EDY} and inductance L_{EDY} respectively. The finite model is that the lossy impedance converged to finite non-zero value as the frequency goes to zero. The detail of this model is explained in the next section. Some noise appeared on the sample response between 7 and 15kHz is caused by incomplete movement

restriction of the loudspeaker membrane / voice coil assembly.

5. FINITE THICKNESS SHORT-RING

The lossy impedance often expressed accurately using the Physical Cauer model. This model is results in the direct discretization of Maxwell's equation without approximation [9], [10], [11], [16]. One type of this model is the LR ladder network and the input impedance components can be yielding the finite real impedance and the inductance at zero frequency. Hence this named the finite model.

The physical reality of a vice coil and surrounding conductive medium (Short-ring) under the normal condition, the R_{EDY} is constrained by the own conductivity and will not be reduced to 0, and the L_{EDY} will not grow infinitely large as the frequency ω goes to 0. This finiteness is not agreed with the conditions given by the equation (2) for R_{EDY} and (3) for L_{EDY}.

Thus to overcome this culprit, the accurate model is developed by the author [18]. Followings are the simplified model using the corner frequency of ω_1, and applied to the expression of the Lossy real impedance R_{VC} and the inductance L_{VC}. The effect of ω_1 is that both R_{EDY} and L_{EDY} converge to a positive non-zero finite value below the frequency ω_1 (23). The lossy impedance's new equations are;

$$R_{EDY} = R_2\sqrt{\frac{\omega_1+\omega}{\omega_0}} \tag{21}$$

$$L_{EDY} = L_3\sqrt{\frac{\omega_0}{\omega_1+\omega}} \tag{22}$$

$$\lim_{\omega\to 0} R_{EDY} = R_2\sqrt{\frac{\omega_1}{\omega_0}}, \lim_{\omega\to 0} L_{EDY} = L_3\sqrt{\frac{\omega_0}{\omega_1}} \tag{23}$$

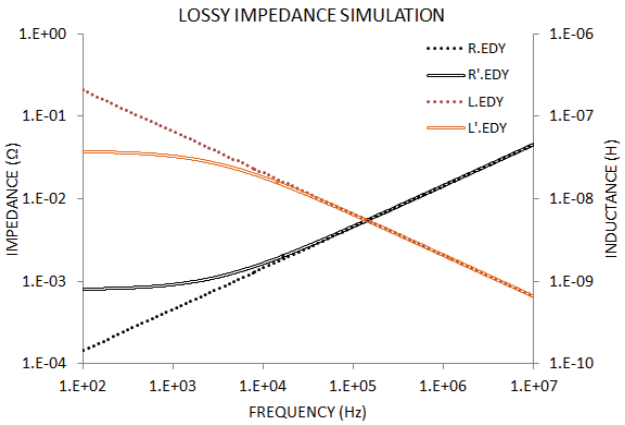

Figure 9 - Lossy resistance and inductance response. Dotted traces are the infinite thickness model, and solid traces are the finite thickness model. R_{EDY} are black traces and L_{EDY} are orange traces.

When the frequency ω is significantly high so that $\omega_1 + \omega \approx \omega$ is held, (21) and (21) yields the same results as the infinite model (2) and (3) respectively. Figure 9 shows the lossy impedance components, R_{EDY} (black) and L_{EDY} (orange). The responses of the infinite model represented by (2) and (3) are shown with dotted traces. The finite model represented by (21) and (22) shown with the solid traces and the both converges a non-zero finite value below ω_1 (5kHz).

6. SIMULATION COMPARISON

Figure 10 shows the real impedance R_{VC}, and Figure 11 shows the inductance L_{VC} frequency responses using three deferent simulation models; Wright, the infinite and the finite model. All three models showed a similar accuracy above 100kHz. At low-frequency range, however, showed some error. The Wright's model (solid black) deviates significantly for the inductance and some visible deviation on the real impedance. The infinite model (dashed blue) resulted in some error on both the real impedance and the inductance. The finite model (solid green) resulted in clear improvement over the infinite model and showed no visible deviation on both the real impedance and the inductance.

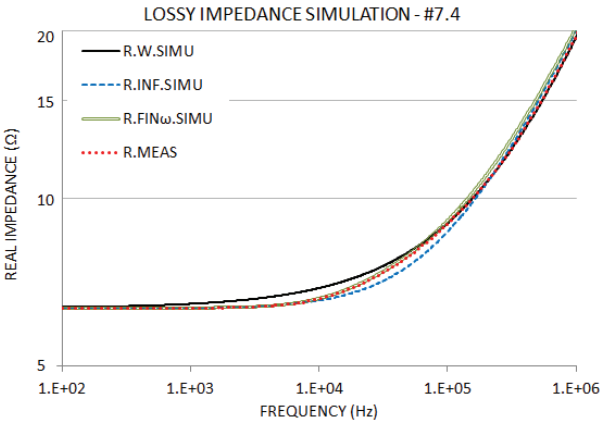

Figure 10 - Real impedance response vs simulations. Sample #7.4 voice coil is dotted-red trace. Simulation traces of; (a) Wright model – black, (b) Infinite model – blue dash and (c) Finite model – green

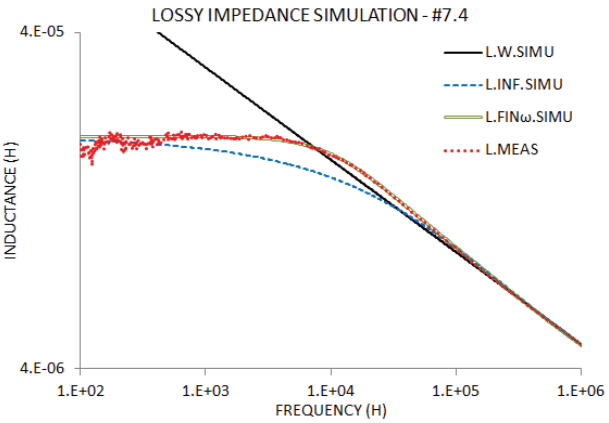

Figure 11 - Inductance response vs simulations. Sample #7.4 voice coil is dotted-red trace. Simulation traces of; (a) Wright model – black, (b) Infinite model – blue dash and (c) Finite model – green

The error function (24) is used to evaluate the simulation accuracy quantitatively. The frequency index denoting as i covers the frequency from 100Hz up to 1MHz. Impedance error ε_Z was obtained using the logarithmic equivalent of the averaged ratio of the impedance difference between the voice coil sample and the simulation, and adjusted by the magnitudes.

Figure 12 shows the simulation error comparison. In this sample, the infinite model reduces the error by approximately 30%, and the finite model reduced the error down to as much as 1/10th of the Wright model for the inductance error of ε_L.

$$\varepsilon_Z = \frac{1}{n}\sum_{i=0}^{n-1} \frac{\left|\log\left(\frac{Z_{ACT(\omega_i)}}{Z_{SIMU(\omega_i)}}\right)\right|}{\log\left(Z_{ACT(\omega_i)} \times Z_{SIMU(\omega_i)}\right)} \qquad (24)$$

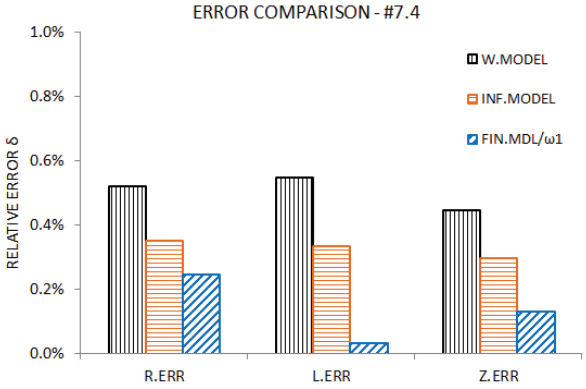

Figure 12 - Test results of three simulation models for sample #7.4: Wright model (black), the infinite model (orange) and the finite model (blue). R.ERR is the real impedance error is ε_R, LERR is the inductance error ε_L and Z.ERR is the total impedance error ε_Z.

7. TEST RESULTS

Impedance and phase responses for three sample loudspeaker voice coils were measured and compared with the finite model simulations are shown in Figures 13 and 14. All simulations agreed with these samples up to 1MHz and beyond for total impedance. For the phase response, samples agreed with the simulations up to 300kHz for sample #6.3, 500kHz for #4.3 and more than 1MHz for sample #3.1. The Wright, the infinite and the finite model simulations error rate are summarized in Table 2. The impedance frequency dependence λ_Z was higher than 0.5 for all samples. The coupling coefficients were calculated to be approximately between 0.8 and 0.95 as shown in Table 3.

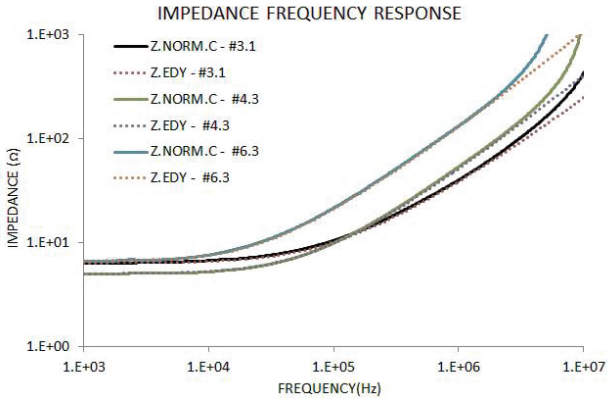

Figure 13 - Impedance response and the simulation comparison: Actual (solid) and simulated data (dot)

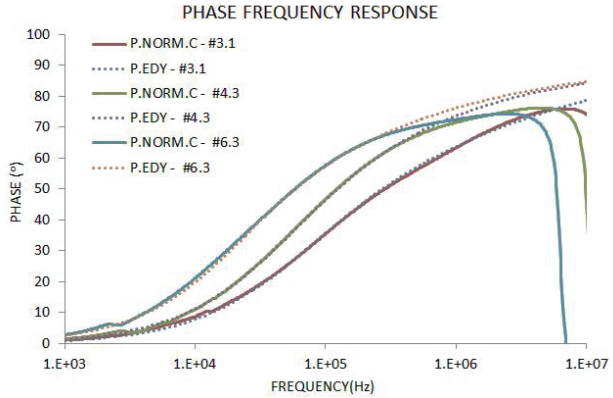

Figure 14 - Phase response and the simulation comparison: Actual (solid) and simulated data (dot)

SIMU. TYPE	ε_R (%)	ε_L (%)	ε_Z (%)
WRIGHT	0.61	0.60	0.53
INFINTE	0.50	0.30	0.35
FINITE	0.25	0.05	0.11
INFINTE / WRIGHT	82.1	49.3	66.5
FINITE / WRIGHT	40.7	7.7	21.4

Table 2 – Five sample average simulation error by simulation type. The last two rows are the relative error to Wright model. ε_R is the real impedance error, ε_L is the inductance error and ε_Z is the total impedance error.

8. CONCLUSION

This paper developed a model describing how the lossy impedance frequency dependence of 0.5 resulted in the total impedance frequency dependence becoming higher than this magnitude. The essential causal mechanism is found to be the less than unit coupling ($\kappa < 1$) of the transformer consisted of the self-inductance L_E and surround conductive medium as the Lossy impedance connected to the secondary winding. The voice coil, by design in the majority of cases, the coupling coefficient κ less than 1 therefore, as shown in earlier sections, the impedance frequency dependence will be higher than 0.5. The finite lossy impedance model resulted in increased accuracy over the infinite model. The inductance simulation error is reduced to 1/6th (0.05/0.30), 1/2 for the

real impedance, and 1/3 for total impedance over the infinite model.

SAMPLE #	R_1 (Ω)	L_1 (uH)	R_2 (mΩ)	L_3 (uH)	N	κ	λ_R	λ_L	λ_Z	ω_1 (kHz)	ω_{SR} (MHz)
#1.2	7.12	52.2	0.09	0.13	67	0.839	0.369	-0.163	0.731	25.1	7.18
#3.1	6.37	18.8	0.13	0.40	37	0.902	0.286	-0.224	0.540	17.7	14.3
#4.3.F	4.97	23.7	0.14	0.36	37	0.931	0.418	-0.276	0.616	35.4	14.7
#6.3.I	6.57	52.2	0.09	0.24	63	0.923	0.415	-0.252	0.621	28.1	10.0
#7.4	6.35	19.6	0.23	0.13	38	0.947	0.392	-0.274	0.588	28.1	20.9

Table 3 - Sample voice coil main parameter and the finite mode simulation results. The real impedance error is denoting as ε_R, the inductance error is ε_L and the total impedance is ε_Z.

REFERENCES

[1] L. Cohen, "The Influence of Frequency on the Resistance and Inductance of Solenoidal Coil", *Bulletin of Bureau of Standard.* P168 ~ 172 (August 1907)

[2] D. R. Holt, "Expansion with Coefficient Algorithms for Time Domain Responses of Skin Effect Lossy Coaxial Cables", *Journal of Research of the national Bureau of Standard.* P156 ~ 159 (March 1970)

[3] J. R. Wright, "An Empirical Model for Loudspeaker Motor Impedance", *AES Journal Vol 38, No 10.* P750 ~ 751 (October 1990)

[4] J. Vanderkooy, "A Model of Loudspeaker Driver Impedance Incorporating Eddy Currents in the Pole Structure", *AES Journal Vol 37, No 3.* P119 ~ 122, P124~126 (March 1989)

[5] K. Thorborg, A. D. Unruh and C. J. Struck. "An Improved Electrical Equivalent Circuit Model for Dynamic Moving Coil Transducers", *AES 122nd Convention.* P4 (2007 May, Austria)

[6] M. Dodd, W. Klippel and J.Oclee-Brown, "Voice Coil Impedance as a Function of Frequency and Displacement", *117th AES Convention.* P3 (San Francisco, 2004 October)

[7] W. M. Leach Jr., "Loudspeaker Voice-Coil Inductance Losses: Circuit Models, Parameter Estimation, and Effect on Frequency Response", *AES Journal Vol 50, No 6.* P444 ~ 446 (June 2002)

[8] S. C. Thompson and D. M. Warren, "Analog circuit model for loudspeakers including eddy current behavior and suitable for time domain simulation", *AES 143rd Convention.* P3 (New York, USA, October 2017)

[9] W.L.A. Neves and H. W. Dommel, "Transformer Core Modeling", *IPST '95 International Conference on Power System Transients.* P125 ~ 126 (Lisbon, September 1995)

[10] C Yen, Z Fazarinc and R.L. Wheeler, "Time-Domain Skin Effect Model for transient Analysis of Lossy Transmission Lines", *Proceeding of the IEEE, Vol 70, No 7.* P750 ~ 753 (July 1982)

[11] L. Colla, S. Lauria and F. Palone, "Finite Sections Modeling of Power Cable System", *The International Conference of Power Systems Transients,* Deft Netherlands, June 2011.

[12] K. Thorborg and C. Futtrup, "Electrodynamic Transducer Model Incorporating Semi-Inductance and Means for Shorting AC Magnetization", *AES Journal of Audio Engineering, Vol 59, No. 9.* P612 ~ 617 (September 2011)

[13] B. Elieli, "The application of inductively coupled shorted turn and the dual-coil loudspeaker system" *AES 83rd Convention.* P3 ~ 5 (New York, October 1987)

[14] I. G. Anazawa, "High Frequency – Ultra Audio Band Mode Voice Coil Temperature Measurement", *142nd AES Convention.* P1 ~ 3 (Berlin Germany, May 2017)

[15] A. Bezzola, et. al., "Variable Fractional Order Analysis of Loudspeaker Transducers: Theory, Simulation, Measurements, and Synthesis", *143rd AES Convention.* P4. (New York, USA, October 2017)

[16] S. Jazebi, et. Al., "Duality-Synthesized Circuit for Eddy Current Effects in Transformer Windings", *IEEE Transaction on Power Delivery*, Vol 28. No 2, April 2013. P2

[17] G. Anazawa, "Impact of Coupling Factor on Lossy Voice Coil Impedance", *AES 146th Convention*, (Dublin, Ireland, 2019 March), P9 Appendix

[18] G. Anazawa, "The Modelling of Finite Thickness Short-ring for Lossy Blocked Voice Coil Impedance", AES 148th Convention, (Vienna, Austria, 2020 May (June))